



Design and Analysis of PV Array with Reduced 7-Level Inverter for Grid Connection

P.Ramesh¹, R.Banupriya² and R.Shivakumar³

¹KET Polytechnic College Krishnagiri – 635203.

²PSV College of Engineering & Technology Krishnagiri.

³Sona College of Technology salem – 636505.

ARTICLE INFO

Article history:

Received: 11 December 2020;

Received in revised form:

13 January 2021;

Accepted: 27 January 2021;

Keywords

Reduced Multilevel Inverters,
PSO.

ABSTRACT

Multilevel inverters are used extensively in many applications due to their increased power rating, improving harmonic performance and reduced electromagnetic interference. However, the usage of more switches in the conventional configuration poses a limitation to its wide range application. This may leads to vast size and price of the inverter is very high. So in order to overcome this problem the new multilevel inverter is proposed with reduced number of switches. The configuration of the PV system is based on the multi-string technology and the maximum power point is obtained using PSO Algorithm. The output of the MPPT tracker controls the duty cycle of the boost converter. To control this power converter, SVPWM based modulation technique is implemented. The results are validated through the harmonic spectrum of the FFT window by using Matlab/simulink.

© 2021 Elixir All rights reserved.

Introduction

The increase in industrialization leads to energy demand. Most of the energy demand is supplied by the fossil fuels. However, increase in air pollution, diminishing fossil fuels and their increasing cost have made it necessary to gaze towards renewable energy sources as a future energy solution. Among these Renewable Energy Sources (RES), solar power systems are the affable solution for electrification. As the solar energy is available in nature and due to its inexhaustible availability, it has become one of the most promising renewable energy. Hence, PV system has been increasingly used in medium sized grid. The increasing use of semiconductors in the high power applications lead to the development of multilevel inverters [1-5]. Multilevel inverters can operate at high switching frequencies with low harmonic distortion. So it is gained more attention in high power application. A multilevel inverter not only achieves high power ratings, but also enables the use of renewable energy sources. Renewable energy sources such as photovoltaic, wind and fuel cells, can be easily interfaced to a multilevel inverter system for high power applications [9].

The Diode clamped, Flying capacitor, Cascaded H-bridge inverter are the three main different multilevel inverter structures which are used in industrial applications with separate dc sources. In flying capacitor and diode-clamped inverter, when the number of semiconductor devices decreases the switching losses also decrease in direct proportion and therefore the efficiency of the entire system increases. For this reason a cascaded multilevel inverter can be considered as an effective option for high medium and high voltage applications. However use of higher level multilevel inverters may impose other problems such as higher number of switching devices, cost complexity etc.

Hence in this work, a topology of 7 level multilevel inverter with reduced number of switching components and reduced number of switching is proposed. The proposed switching configuration gives almost sinusoidal output voltage. Therefore the harmonic content as well as distortion factor are reduced.

Proposed Methodology

The Configurations of a proposed system is shown in Figure 1.

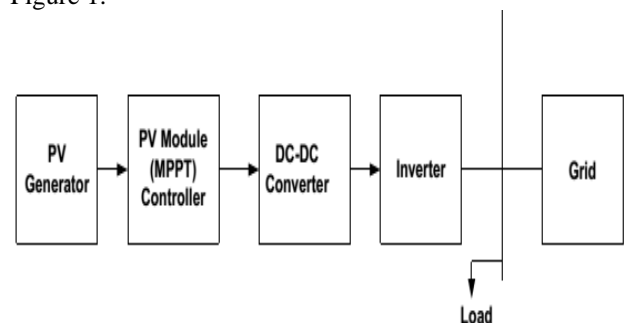


Figure 1. Block Diagram of a PV and grid

As the photovoltaic power varies with the climatic conditions, to obtain the maximum power from PV array, it is coupled with a Maximum Power Point Tracker (MPPT). As the photovoltaic energy sources generate power at variable low dc voltage, it requires power conditioning. For this purpose, DC-DC converter is used. The output obtained from the DC-DC converter is coupled to the inverter [7].

Modeling of PV Array

The building block of PV arrays is the solar cell. It is basically a p-n junction which directly converts light energy into electricity. The equivalent circuit of a PV cell is shown in Figure 2.

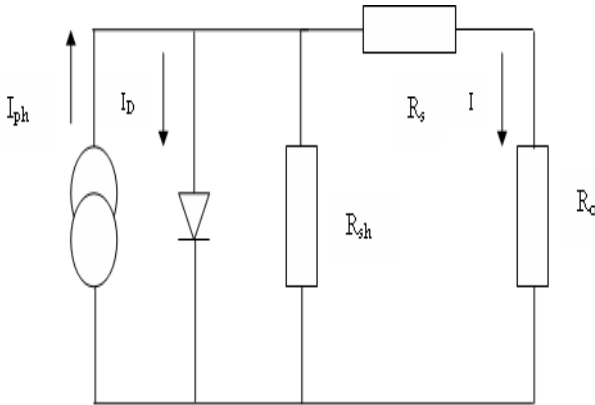


Figure 2. Equivalent circuit of a PV cell

PV cells grouped in large unit forms a PV module and are connected in series-parallel configuration to form PV array. The mathematical model of a PV array is represented by the equation:

$$I = n_p I_{ph} - n_p I_{rs} \left[\exp\left(\frac{q}{KTA}\right) * (V / n_s) - 1 \right] \quad (1)$$

where

- I_{ph} - photo current
- I - output current of PV array
- V - output voltage of PV array
- n_s - number of cells in series
- n_p - number of cells in parallel
- q - charge of an electron
- K - Boltzmann's constant [8.62 x 10⁻⁵ eV/K]
- A - ideality factor of the p-n junction. It ranges between 1-5.
- T - cell temperature (K)
- I_{rs} - cell reverse saturation current.

The cell reverse saturation current I_{rs} varies with temperature according to the following equation:

$$I_{rs} = I_{rr} \left[\frac{T}{T_r} \right]^3 \exp\left(\frac{qE_G}{KA} \left[\frac{1}{T_r} - \frac{1}{T} \right] \right) \quad (2)$$

Where T_r is the reference temperature, I_{rr} is the reverse saturation temperature at T_r and E_G is the band gap of the semiconductor used in the cell.

The photo current I_{ph} depends on the solar radiation and cell temperature as follows:

$$I_{ph} = [I_{scr} + K_i(T - T_r)]s / 100 \quad (3)$$

Where I_{scr} is the short-circuit current at reference temperature 2.52A], K_i is the short circuit current temperature coefficient and s is the solar radiation in mW/cm³. Thus the calculated PV power can be given as

$$P = IV = n_p I_{ph} V \left[\frac{q}{KTA} * (V / n_s) - 1 \right] \quad (4)$$

The operation of PV system varies according to the weather condition. Hence a dynamic tracking system is required to obtain maximum power from the PV array.

Maximum Power Point Tracker

A typical solar panel converts only 30 to 40 percent of the incident solar radiation into electrical energy. Hence in order to improve the efficiency of the solar panel Maximum Power Point Tracking technique is implemented [1-5].

Maximum Power Point Tracker frequently referred as MPPT is an electronic system that operates the PV modules to produce maximum power. MPPT varies the electrical operating point of the modules so that the modules are able to deliver maximum power.

The MPPT maximizes the power produced by the panels by controlling the voltage and current of PV system. The PV output current and voltage are measured using a current

sensor at the PV output terminal. From the measured voltage and current value the output power of PV is calculated. This power extraction control is necessary because the Maximum Power Point (MPP) of a solar panel varies with the radiation and temperature.

MPPT Algorithm

Particle Swarm Optimization

The Particle Swarm Optimization (PSO) was first developed by Kennedy (1995). It is a population based optimization technique, motivated by biological concepts like swarming and flocking. The basic idea behind PSO emerged from the behavior observed among flocks of birds, schools of fish or swarms of bees. The salient features of PSO are its easy implementation, its high speed convergence and non-requirement of gradient information. An extensive range of different optimization problems can be solved by this technique. PSO is initialized with the population, which is randomly generated and it always conducts a search in the population of particles. Every particle in the population represents a possible candidate solution (fitness) to the given problem. In a PSO system, the search towards optima is carried out in a multidimensional search space. The particles can move through the search space and make changes in its position by having the information such as (i) the distance between the current position of the particle and *Pbest*, (ii) the distance between the current position of the particle and *Gbest*. Every particle memorizes its best solution in addition to its position achieved so far and is known as *Pbest*, the Personal best. It also knows the best value along with its position found in the group among *Pbests*, known as *Gbest*, the Global best. The basic theory of PSO insists on accelerating each particle on the road to its *Pbest* and the *Gbest* locations. Concept of particle position modification in PSO is shown in Figure 3.

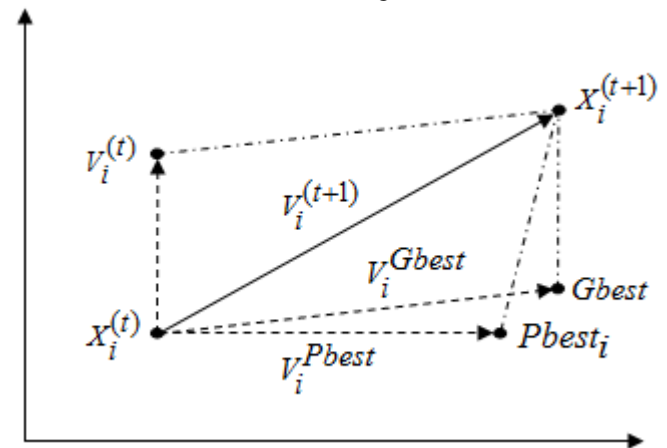


Figure 3. Concept of particle position modification in PSO

where V_i^{Pbest} is the velocity based on *Pbest* and

V_i^{Gbest} is the velocity based on *Gbest*.

In n dimensional search space, every particle in the population can be a potential solution to a given problem. The position of the i^{th} particle is then represented as $X_i = (x_{i1}, x_{i2}, \dots, x_{in})$. A particle i is moving through a search space with a velocity that corresponds to $V_i = (v_{i1}, v_{i2}, \dots, v_{in})$.

Let $Pbest$ and $Gbest$ of the i^{th} particle be given as $Pbest_i = (x_{i1}^{Pbest}, x_{i2}^{Pbest}, \dots, x_{in}^{Pbest})$ and $Gbest = (x_1^{Gbest}, x_2^{Gbest}, \dots, x_n^{Gbest})$. In PSO, the velocity of the individual particle i is updated using the following equation (5).

$$V_i^{(t+1)} = \omega \times V_i^{(t)} + c_1 \times r_1 \times (Pbest_i - X_i^{(t)}) + c_2 \times r_2 \times (Gbest - X_i^{(t)}) \quad (5)$$

where

$V_i^{(t)}$ velocity of the i^{th} particle at iteration t ,

t pointer of iterations (generations),

ω inertia weight factor, that is used to control the impact of the previous velocity over the new velocity,

c_1, c_2 acceleration coefficients, where c_1 and c_2 are positive constants called as coefficient of self-recognition component and coefficient of social component,

r_1, r_2 random numbers equally spread within the range [0, 2],

$X_i^{(t)}$ position of the particle i at iteration t ,

$Pbest_i$ best position of particle i until iteration t ,

$Gbest$ best position of the group until iteration t .

The predefined values of the acceleration coefficient c_1, c_2 and inertia weight ω are substituted in the equation (2.4) and random numbers r_1, r_2 are uniformly generated within the limit [0, 2] in order to calculate the new velocity. The inertia weight ω is calculated by the equation (6)

$$\omega = \omega_{\max} - \frac{\omega_{\max} - \omega_{\min}}{Iter_{\max}} \times Iter \quad (6)$$

where

ω_{\max} initial weight

ω_{\min} final weight

$Iter_{\max}$ maximum iteration number

$Iter$ current iteration number

Hence, a new velocity which is used to perform a shift in the current searching point in the direction of $Pbest$ and $Gbest$ is calculated. Each particle tries to move from the current position to the new one by using the modified velocity, which is given by the equation (7):

$$X_i^{(t+1)} = X_i^{(t)} + V_i^{(t+1)} \quad (7)$$

Finally, in PSO all the particles are trying to move about better positions. By the combined effort of the whole population, the best position (optimum solution) can be obtained.

The flowchart the PSO algorithm for MPPT is shown in Figure 4.

Thus, a maximum power point tracker achieves maximum power from the solar PV module. A non isolated DC-DC converter (step up/ step down) is implemented for conversion of this maximum power to the grid. The MPPT controller controls the output voltage of the DC-DC converter

by regulating the PWM signals applied to the switch of the inverter unit.

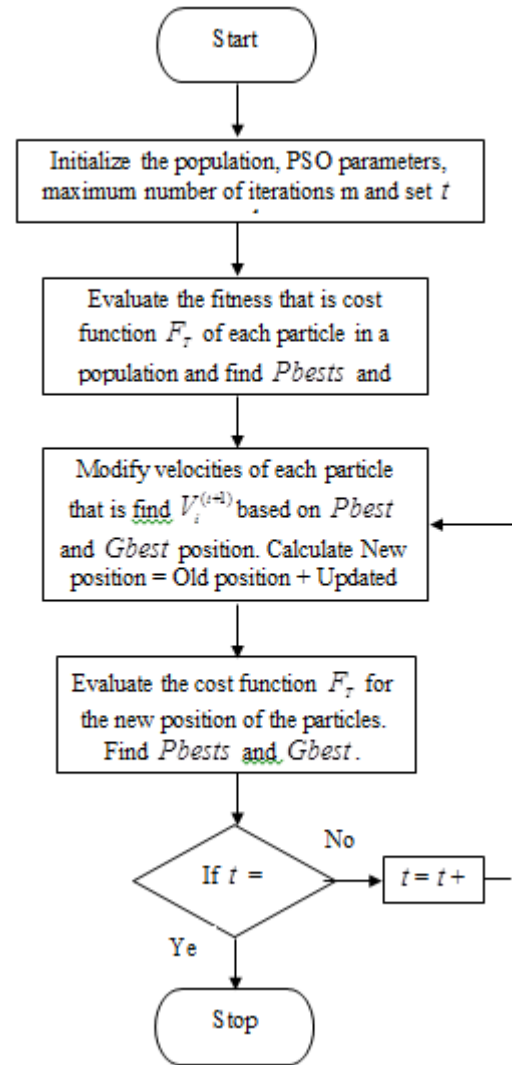


Figure 4. Flowchart of the PSO algorithm Boost Converter

The DC-DC step-up/step down (Buck-Boost) converter circuit regulates the output voltage of the PV module. The step-up converter configuration with a low duty-cycle value allows the converter to operate with small power losses.

DC/AC Inverter

A DC/AC inverter is a device that converts electrical power from DC to AC. Multilevel inverters (MLI) are recently used in high power applications. Moreover, three different major multilevel converter structures such as cascaded H-bridges converter with separate dc sources, diode clamped (neutral-clamped), and flying capacitors (capacitor clamped) have been reported in the literature.

Among these structures, diode clamp inverter has the capability to reduce the harmonic content and decrease the voltage or current ratings of the semiconductors.

Design of inverters

Conventional Topology.

Using 3 DC voltage sources, 3 H-bridge units each with 4 switches together forming 12 switches in total are used in conventional CMLI which is represented in Figure 5. General expression for output voltage levels, where is the number of switches in the configuration. Each Bridge is outputting 3 Levels, $+V_{dc}$, 0 , $-V_{dc}$. Cascading 3 Bridges in such a fashion to produce stepped 7 level staircase waveforms.

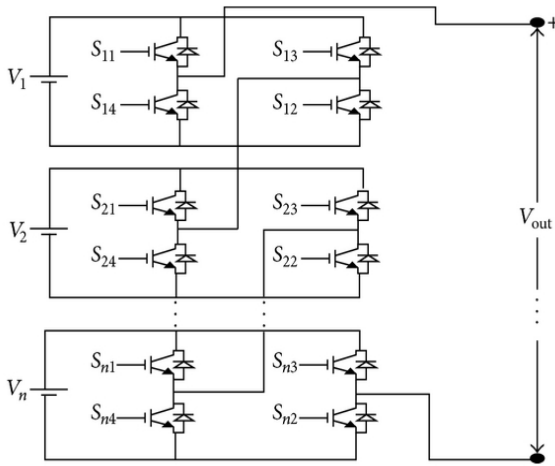


Figure 5. Conventional cascaded 7-level MLI.

Proposed Topology
7-Level, 9 Switches.

This topology which is shown in Figure 6 is built with 3 dc sources, 1 H-bridge composed of 4 switches and then additional 5 more switches for producing stepped 7 levels, for positive and negative half cycles.

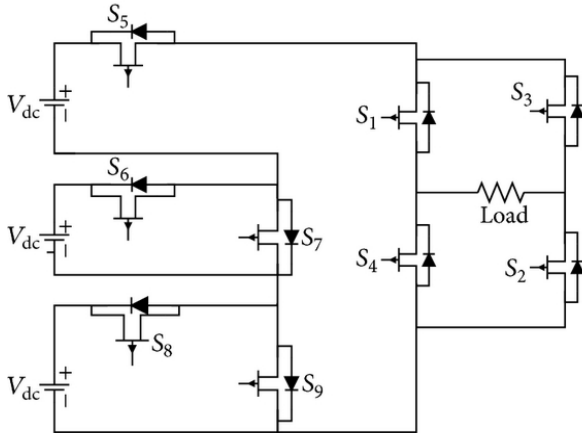


Figure 6. 7-level 9-switch topology.

Space Vector Modulation

The space vector concept, which is derived from the rotating field of induction motor, is used for modulating the inverter output voltage. In this modulation technique the three phase quantities can be transformed to their equivalent two-phase quantity either in synchronously rotating frame (or) stationary frame. From these two-phase components, the reference vector magnitude can be found and used for modulating the inverter output. The process of obtaining the rotating space vector is explained in the following section, considering the stationary reference frame. Considering the stationary reference frame let the three-phase sinusoidal voltage component be,

$$V_a = V_m \sin \omega t$$

$$V_b = V_m \sin(\omega t - 2\pi/3)$$

$$V_c = V_m \sin(\omega t - 4\pi/3)$$

When this three-phase voltage is applied to the AC machine it produces a rotating flux in the air gap of the AC machine. This rotating resultant flux can be represented as single rotating voltage vector. The magnitude and angle of the rotating vector can be found by means of Clark's Transformation as explained below in the stationary reference frame. To implement the space vector PWM, the voltage the stationary dq reference frame that consists of the horizontal (d) and vertical (q) axes as depicted in Figure 5.

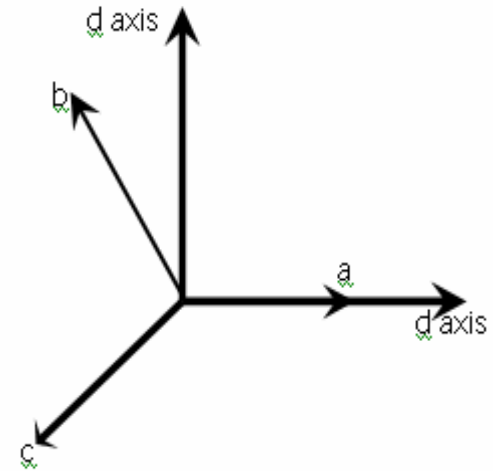


Figure 7. The relationship of abc reference frame and stationary dq reference frame.

As described in Figure 6, the transformation is equivalent to an orthogonal projection of $[a \ b \ c]^T$ onto the two-dimensional perpendicular to the vector $[1 \ 1 \ 1]^T$ (the equivalent d-q plane) in a three-dimensional coordinate system. As a result, six non-zero vectors and two zero vectors are possible. Six non-zero vectors (V_1 - V_6) shape the axes of a hexagonal as depicted in Figure 6, and supplies power to the load. The angle between any adjacent two non-zero vectors is 60 degrees. Meanwhile, two zero vectors (V_0 and V_7) are at the origin and apply zero voltage to the load. The eight vectors are called the basic space vectors and are denoted by ($V_0, V_1, V_2, V_3, V_4, V_5, V_6, V_7$). The same transformation can be applied to the desired output voltage to get the desired reference voltage vector, V_{ref} in the d-q plane. The objective of SVPWM technique is to approximate the reference voltage vector V_{ref} using the eight switching patterns. One simple method of approximation is to generate the average output of the inverter in a small period T to be the same as that of V_{ref} in the same period

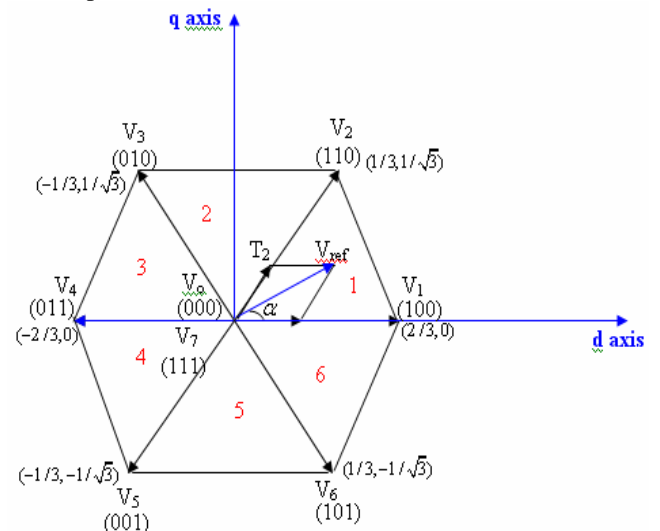


Figure-8. Basic switching, vectors and sectors.

Switching States

Computed Results and Discussion

A seven CHB MLIs are simulated in MATLAB-Simulink and a detailed performance analysis is done in terms of harmonic contents. The simulation study is carried out in MATLAB environment to verify the proposed control approach. The output of the boost converter is shown in figure 7. Figure 8 shows the output voltage waveform of the proposed inverter.

Table 1. Switching patterns and output vectors.

Sl.NO	S1	S2	S3	S4	S5	S6	S7	S8	S9	Output voltage
1	ON	ON	ON	OFF	ON	OFF	ON	OFF	ON	+Vdc
2	ON	ON	OFF	OFF	ON	ON	OFF	OFF	ON	+2Vdc
3	ON	ON	OFF	OFF	ON	ON	OFF	ON	OFF	+3Vdc
4	OFF	OFF	OFF	OFF	OFF	OFF	OFF	OFF	OFF	0
5	OFF	OFF	ON	ON	OFF	ON	OFF	ON	OFF	-Vdc
6	OFF	OFF	ON	ON	OFF	OFF	ON	ON	OFF	-2Vdc
7	OFF	OFF	ON	ON	OFF	OFF	ON	OFF	ON	-3Vdc

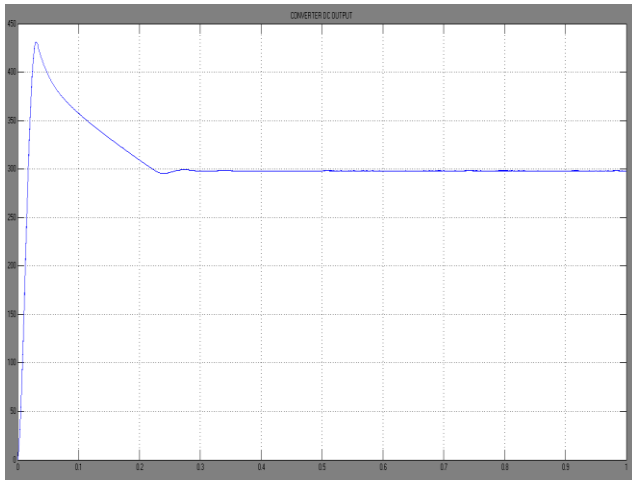


Figure 7. Output voltage of the converter.

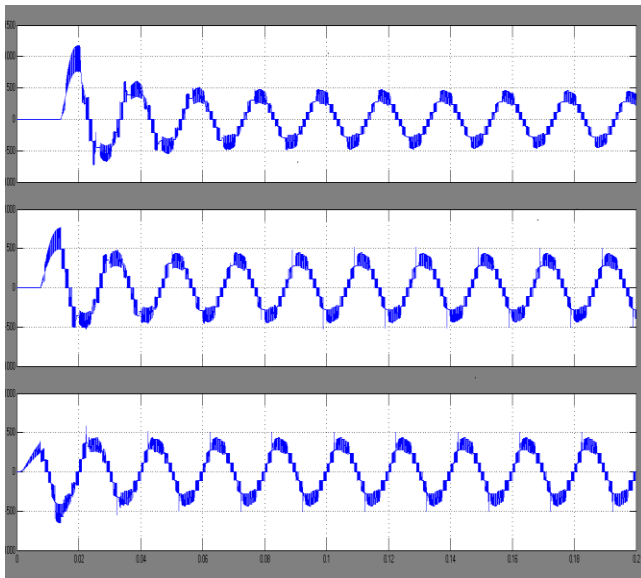


Figure 8. Voltage wave form of inverter.

Table 6. Voltage stress in proposed topology across switches.

Parameter	Conventional CMLI	9switches, 7-level
Voltage stress	5 V (All switches)	11 V (S5) 10 V (S6) 2 V(S7) 10 V (S8 &S9)

System Analysis

The efficiency of the proposed system is analyzed in terms order of harmonics.

THD Analysis

Figure 10 illustrate plots of the order of harmonics versus magnitude of grid voltage. With the proposed system, the order of harmonics is less than 5%. The Fast Fourier Transform (FFT) is used to measure the order of harmonics.

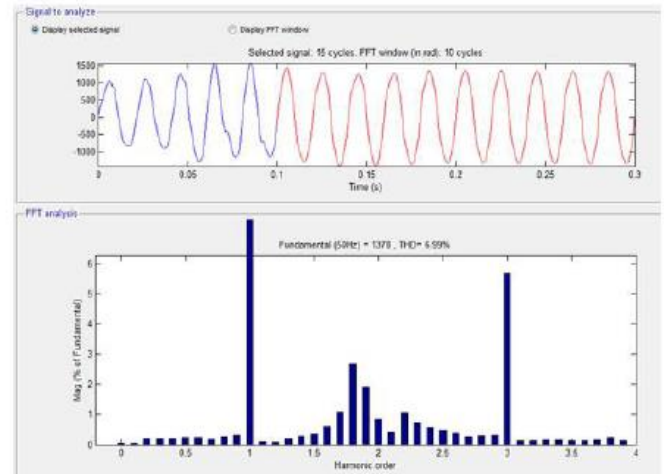


Figure 9. Harmonic spectrum of Grid voltage

From the Figure 9, it is concluded that the total harmonic distortion (THD) of the voltage is improved to 6.99% which is within the acceptable limit of IEEE 519 standard for voltage distortions in distribution system. Thus from the simulation results, it is evident that this method can be efficiently used for harmonics reduction along with injection of active power from solar system.

Conclusion

Thus, a seven level cascaded H-bridge multilevel inverter with reduced switch is simulated using the MATLAB/SIMULINK with PV cell as one DC source and its performance in reducing THD is analyzed. From the simulated analysis, It is observed that the output voltage of proposed seven level inverter is close to sinusoidal wave form when compared with conventional multilevel inverter. It can also observe that the quality of voltage wave form increases with increase in voltage levels. Also the SPWM technique controlled the inverter to produce seven levels in the output waveform. The main advantage of this novel topology is that the number of switching devices required is reduced leading to less cost, less losses and easy control in addition to fewer harmonic.

References

1. J. Rodríguez, J.-S. Lai, and F. Z. Peng, "Multilevel inverters: a survey of topologies, controls, and applications," IEEE Transactions on Industrial Electronics, vol. 49, no. 4, pp. 724–738, 2002.
2. D. Mohan and S. B. Kurub, "Performance analysis of SPWM control strategies using 13 level cascaded MLI," in IEEE International Conference on Advances in Engineering Science & Management (ICAESM '12).
3. O. L. Jimenez, R. A. Vargas, J. Aguayo, J. E. Arau, G. Vela, and A. Claudio, "THD in cascade multilevel inverter symmetric and asymmetric," in Proceedings of the IEEE Electronics, Robotics and Automotive Mechanics Conference (CERMA '11), pp. 289–295, November 2011.

4. P. Palanivel and S. S. Dash, "Analysis of THD and output voltage performance for cascaded multilevel inverter using carrier pulse width modulation techniques," *IET Power Electronics*, vol. 4, no. 8, pp. 951–958, 2011.
5. J. J. Nedumgatt, D. Vijayakumar, A. Kirubakaran, and S. Umashankar, "A multilevel inverter with reduced number of switches," in *Proceedings of the IEEE Students' Conference on Electrical, Electronics and Computer Science (SCEECS '12)*, pp. 1–4, March 2012.
6. I. Houssamo, F. Locment, M. Sechilariu, "Maximum power tracking for photovoltaic power system: Development and experimental comparison of two algorithms". *Renewable Energy*, vol. 35, No 10, pp. 2381-2387, 2010. [4] I. H. Altasa, A. M. Sharaf, "A novel maximum power fuzzy logic controller for photovoltaic solar energy systems". *Renewable Energy*, vol. 33, No 3, pp. 388-399, 2008.
7. Syafaruddin, E. Karatepe, T. Hiyama, "Polar coordinated fuzzy controller based real-time maximum-power point control of photovoltaic system". *Renewable Energy*, vol. 34, no 12, pp. 2597-2606, 2009.
8. C. Larbes, S. M. A. Cheikh, T. Obeidi, A. Zerguerras, "Genetic algorithms optimized fuzzy logic control for the maximum power point tracking in photovoltaic system". *Renewable Energy*, vol. 34, No 10, pp. 2093-2100, 2009.
9. T. Tafticht, K. Agbossou, M. L. Doumbia, A. Chériti, "An improved maximum power point tracking method for photovoltaic systems". *Renewable Energy*, vol. 33, No 7, pp. 1508-1516, 2008.
10. A. Chaouachi, R. M. Kamel, K. Nagasaka, "A novel multi-model neuro-fuzzy-based MPPT for three-phase grid-connected photovoltaic system". *Solar Energy* 2010;84(12):2219-2229.
11. N. Hamrouni, M. Jraidi, A. Chérif, "New control strategy for 2-stage grid-connected photovoltaic power system". *Renewable Energy*, vol. 33, no 10 pp. 2212-2221, 2008.
12. S-K Kim, J-K Jeon, C-H Cho, E-S Kim, J-B Ahn, "Modeling and simulation of a grid-connected PV generation system for electromagnetic transient analysis". *Solar Energy*, vol. 83, No 5, pp. 664-678, 2009.
13. Gobinath.K, Mahendran.S, and Gnanambal.I "New cascaded H-bridge Multilevel Inverter with Improved Efficiency" *International Journal of Advanced Research in Electrical, Electronics and Instrumentation Engineering*, April 2013.
14. W. Xiao, F. F. Edwin, G. Spagnuolo, J. Jatsvevich, "Efficient approach for modelling and simulating photovoltaic power system " *IEEE Journal of photovoltaics*.. vol. 3,no. 1, pp. 500-508,Jan. 2013.